# STUDY OF AIR DISTRIBUTION PHASES OF THE SMALL-SIZED ROTARY VANE VACUUM PUMP

Elchyn ALIIEV [1], Vladimir DUDIN [2], Alexandr YANOVSKY [3]

*For mobile equipment (for example, individual milking machines), there is a need to develop small-sized vacuum pumps (specific gravity not higher than 0.6 kg/(m³/h)) with the required high throughput capacity (not less than 20 m³/h) and low specific energy consumption (not above 0.5 kW h/m³) to create a stable vacuum pressure in the equipment system at the level of 50-60 kPa. Rotary vane vacuum pumps meet these requirements. A well-known simplified technique for determining the phases of air distribution and accordantly the location and geometrical dimensions of the intake and discharge port of rotary vane vacuum pumps is used only for the case of the radial arrangement of the grooves of the plates. Therefore, the article solves the scientific problem of determining the influence of the design and technological parameters of a small-sized rotary vane vacuum pump for mobile equipment (for example, individual milking machines) on the efficiency of its operation. The actual novelty is the improvement of the methodology for determining the parameters of the air distribution phases in small-sized rotary vane vacuum pumps with an inclined arrangement of the plates and testing it experimentally. According to the results of analytical research, numerical modeling, and experimental research the regularities of pressure change in the working chamber of the rotary vane vacuum pump with the inclined arrangement of plates depending on a rotor angle of rotation are received and their comparison is carried out.*

**Keywords**: rotary vane vacuum pump, phases, vacuum pressure, investigation, modeling, experiment.

## 1. Introduction

Rotary vane vacuum pumps in comparison with other types of mechanical pumps have a high mechanical efficiency, which characterizes the ratio of indicator power to power on the pump shaft, equal to 0.8–0.9 [1]. Pumps of this type are well balanced, at rather big turns create smaller pulsations of vacuum

[1] Doctor of Engineering Science, Senior Researcher, Director, Institute of Oilseed Crops of the National Academy of Agrarian Sciences of Ukraine, Ukraine, e-mail: aliev@meta.ua
[2] Candidate of Technical Sciences, Associate Professor, Head of Department, Engineering and Technology Faculty, Dnipro State Agrarian and Economic University, Ukraine, e-mail: vladudin@i.ua
[3] Candidate of Physics and Mathematics, Associate Professor, Department of General and Applied Physics, Zaporizhia National University, Ukraine, e-mail: yanovskyas@gmail.com

pressure and have small overall dimensions and weight. They consist of fewer parts; they do not have suction and discharge valves [2]. In addition, they are distinguished by a simplified scheme of air distribution [3]. Rotating vacuum pumps do not require massive foundations, because they have a smooth, with minimal vibration, nature of work. These pumps pump air more evenly and are faster [4].

Pumps of different brands differ from each other by the location of the rotor in the housing, the cross-section of the inlet and outlet pipes, the location of windows in the housing, rotor speed, plate material, mounting the drive on the frame, geometric dimensions, weight, and actual productivity [5–7].

Most rotating vacuum pumps have a lateral or bottom rotor location. Depending on the required productivity, the pumps produce different power by using different modes and speeds of the rotor, but, despite this, they have a high level of unification [8]. However, for a mobile device (for example, individual milking machines) there is a need to create small vacuum pumps (specific weight – not more than 0.6 kg/($m^3$/h)) with the required high throughput (not less than 20 $m^3$/h) and low specific energy consumption (not more than 0.5 kW h/$m^3$) in order to obtain a stable vacuum pressure in the equipment system at the level of 50–60 kPa.

As for the disadvantages of rotary vane vacuum pumps, it is, at first the presence of friction surfaces that require lubrication. At the same time, oil is thrown out into the atmosphere, worsening also environmental friendliness of the pump. In addition, they have a low pumping coefficient and high specific energy consumption, which is obviously due to air losses (due to overflow) and energy costs to overcome friction [9]. The gradual decrease in the performance of rotary vane vacuum pumps during operation is due to the wear of the main parts and, therefore, – an increase in internal radial and end air flows. In the new pump, the end flows prevail over other internal flows and reach 50-60 %, but during the exploitation is a significant increase in the share of radial flows, they become decisive [10].

Consider the reasons for the increase in gas flows. Suction, compression, and injection of gas, in pumps of this type, are carried out by changing the volume of the chambers, consisting of an eccentrically located rotor, plates, housing, and caps of the pump. The tightness of the chambers from the end is provided by small gaps between the rotor and the side covers, in the radial direction – a plate, which under the action of centrifugal force is pressed against the pump housing. Their wear occurs because of sliding friction of the contact surfaces, and, depending on the conditions, there may be dry, boundary, and semi-liquid friction [11].

After entering the operating mode, the friction of the vapors of the pump work in conditions of semi-liquid friction. This type of friction is characterized by

the simultaneous presence of liquid and marginal lubrication. With this type of friction, the liquid oil layer is displaced in places, and the friction surfaces come into contact [12]. At the contact points of the surfaces, there is more intense wear than at the places separated by a layer of grease, the plates begin to wear unevenly, and the friction surface becomes wavy, while the contact area in the friction vapors decreases, specific loads and temperature increase, which further intensifies the wear process. In addition, it should be noted that the oil is preferably fed to the pump from the end caps by injection, as a result, the distribution of lubrication along the stator length of the pump is uneven, especially in transient modes (start-stop) of the pump. This leads to uneven wear of the plates, their skew in the groove of the rotor, and jamming [13].

Another cause of increased wear on pump parts is dust that is sucked in with the air as well as wear products – this leads to abrasive friction. The abrasive, getting on an oil surface, stick to it, and in some cases and is taken in it therefore in a contact zone there is the scoring of friction surfaces. This mostly applies to the housing, side covers, and plates of the pump, on the working surface of which scratches and burrs are formed, which leads to a decrease in the density of the couplings. The elevated temperature in the friction vapors promotes drying and delamination of the plates. Oxidative processes also have a certain effect on the intensity of wear – under the influence of the environment, oxide films are formed, which are easily destroyed during friction and then reappear. At the same time the plates, both on height, and on length have the greatest wear.

According to our previous studies [9-12], the most effective way to reduce the friction power of the plates is to increase the height of the plates. With a constant eccentricity value, without reducing the performance of the vacuum pump and without increasing its overall dimensions, an increase in the plate height can significantly reduce the friction power. The main way to increase the depth of the groove is the use of inclined grooves in the rotor of a small-sized vacuum pump, which is a constructive and technical novelty [14].

In a review of the studies [15–20] on the investigation of the efficiency of rotary vane vacuum pumps, it was found that the main factor that affected the process of its operation are the air distribution phases. It is known that vacuum pumps have a degree of compression that does not exceed three units and therefore the phases of air distribution should be chosen considering possible air flows because even in geometrically close machines the flow rate varies between 0.3–0.9 and depends on the flow rate and heating factor. Therefore, incorrectly selected phases of air distribution, shape, and section of input and output and nozzles adversely affect the working process of the pump, its temperature, and excess air pressure at the outlet of the pump. A simplified technique for determining of the air distribution phases and accordantly the location and geometrical dimensions of the intake and discharge port of rotary vane vacuum

pumps is known [15-20]. This technique is only used for rotary vane vacuum pumps with radial plate slots. Therefore, the aim of the research is to develop a methodology for calculating the phases of air distribution, the location and dimensions of the intake and discharge port of a small-sized vane rotary vacuum pump with an inclined arrangement of the plates.

## 2. Results of analytical research

The phases of air distribution of rotary vane vacuum pumps (Fig. 1) are characterized by the following indicators: suction angle $\alpha_{in}$ – characterizes the size of the suction window; full compression angle $\alpha_p$ – characterizes the angle of rotation of the rotor relative to the pump housing from the endpoint of the suction to the starting point of the injection; release angle $\alpha$ – characterizes the dimensions of the injection window; injection angle $\alpha_{out}$ – the angle between the lower edge of the injection window and the point of minimum clearance between the rotor and the stator; the angle of harmful space $\delta$ – is the sum of the angles of compression of the clamped volume $\delta_1$ and reverse expansion $\delta_2$; the suction end angle $\varphi_{in}$ is the sum of the angles of harmful space $\delta$ and suction $\alpha_{in}$. In this case: $\varphi$ is the angle of rotation of the rotor (bisectors of the angle $\beta$ between adjacent plates that form the working chamber), $\psi$ is the angle of inclination of the plates.

The location and size of the suction and discharge windows are selected based on the following considerations. The position of the lower edge of the suction window is chosen so that the opening of the working chamber with the suction pipe occurs now when the volume of the working chamber reaches the maximum value. The position of the upper edge of the suction window must be selected from the condition of equality of pressure in the working chamber and the pipe at the initial moment of suction. The position of the lower edge of the injection window is selected from the same condition, but at the beginning of the injection. The position of the upper edge of the discharge window must correspond to the minimum volume of the chamber at the end of injection.

In determining the phases of air distribution, we rely on the dynamics of changes in the volume of the working chamber and the pressure in it. We have proposed a solution to the problem by calculating the cross-sectional area $S(\varphi)$ of the working chamber of a rotary vane vacuum pump with an inclined arrangement of plates depending on the angle of rotation of the rotor $\varphi$, the solution of which is illustrated in Fig. 2.

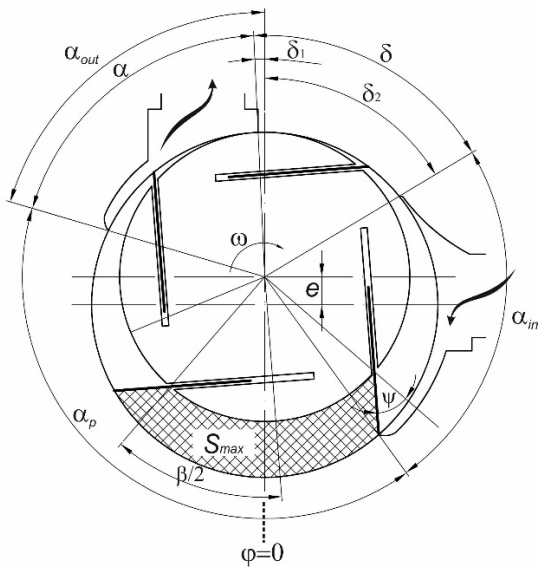


Fig. 1. Scheme for determining the phases of air distribution in a rotary vane vacuum pump with an inclined arrangement of plates

$$S(\varphi)=\frac{1}{2}\left(x_A-r_0+e\cos\omega t\right)\sqrt{R^2-\left(x_A-r_0-e\cos\omega t\right)^2}-\frac{1}{2}\left(e\cos\omega t-r_0\right)\times$$
$$\times\sqrt{R^2-\left(r_0+e\cos\omega t\right)^2}+\frac{R^2}{2}\left[\arcsin\frac{x_A-r_0-e\cos\omega t}{R}+\arcsin\frac{r_0+e\cos\omega t}{R}\right]- \qquad (1)$$
$$-\frac{1}{2}\left[\left(x_A-r_0\right)\sqrt{r^2-\left(x_A-r_0\right)^2}+r_0\sqrt{r^2-r_0^{\,2}}\right]-\frac{r^2}{2}\left[\arcsin\frac{x_A-r_0}{r}+\arcsin\frac{r_0}{r}\right]+$$
$$+e\sin\omega t\cdot x_A+\frac{1}{2}\left(x_B-r_0+e\cos\omega t\right)\sqrt{R^2-\left(x_B-r_0-e\cos\omega t\right)^2}-$$
$$-\frac{1}{2}\left(x_A-r_0+e\cos\omega t\right)\sqrt{R^2-\left(x_A-r_0-e\cos\omega t\right)^2}+\frac{R^2}{2}\left[\arcsin\frac{x_B-r_0-e\cos\omega t}{R}+\right.$$
$$\left.+\arcsin\frac{x_A-r_0-e\cos\omega t}{R}\right]+\left(e\sin\omega t\cdot x_A-r_0\right)\left(x_B-x_A\right),$$

where t – is the time, s; $x_A=r_0^2+\sqrt{0{,}5r_0^2+r^2-2r_0^2}$ – distance to the characteristic point A of the cross-section of the pump chamber, m; $r_0=r\sin\psi$ – radius of the circle to which all the plates are tangent, m; $x_B=r_0+e\cos\varphi+\sqrt{\left(r_0+0{,}5e\cos\varphi\right)^2+\left(R^2-2r_0^2-2r_0e(\cos\varphi-\sin\varphi)-e^2\right)}$ – distance to the characteristic point B in the cross-section of the pump chamber, m;

r – is the radius of the rotor, m; R – is the radius of the stator, m; e – eccentricity, m; φ – rotor rotation angle; ω is the rotor rotational speed, $s^{-1}$.

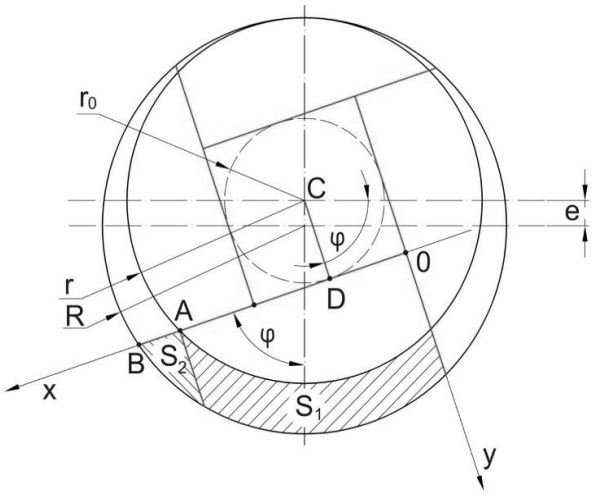


Fig. 2. Calculation scheme for determining the cross-sectional area of the working chamber

Referred to Fig. 3 the dependence of the pressure changes in the working chamber $P(\varphi) = P_{cr} \cdot (S(\varphi_A)/S(\varphi))^{\gamma}$ ($P_{st}$ – gas pressure at the beginning of compression, kPa; γ – polytrope index) suggests that its connection with the discharge window (point A) should occur at an angle of 76°, and the beginning of suction – 187.4° (point B). The moment of disconnection of the working chamber with the discharge window will correspond to the angle of rotation of the rotor 222.5°, at which there is a complete transition of the working chamber from the compression side to the suction side (point C). Point B characterizes the moment of transition of the first during rotation of the plate from the injection side to the suction side (passing the point of the smallest radial gap between the rotor and the stator), i.e., the division of the working chamber into two parts. In the first half of the chamber (segment B-C-D) the vacuum pressure increases, and in the second pressure is equal to the discharge pressure (segment B-C). Point E corresponds to the angle of rotation of the rotor 347.3°, at which the volume of the working chamber becomes the most important and is detached from the suction window.

According to Fig. 1, the positions of the contact points for the first and second along the rotation of the plates with the stator are characterized by the values of angles 1 and 2. Given this, the position of the contact points of the plates relative to the angle can be determined using the math expressions $\varphi_1 = \varphi + (0{,}5\beta + \gamma_1)$, $\varphi_2 = \varphi - (0{,}5\beta - \gamma_2)$ for the first and second plates, respectively.

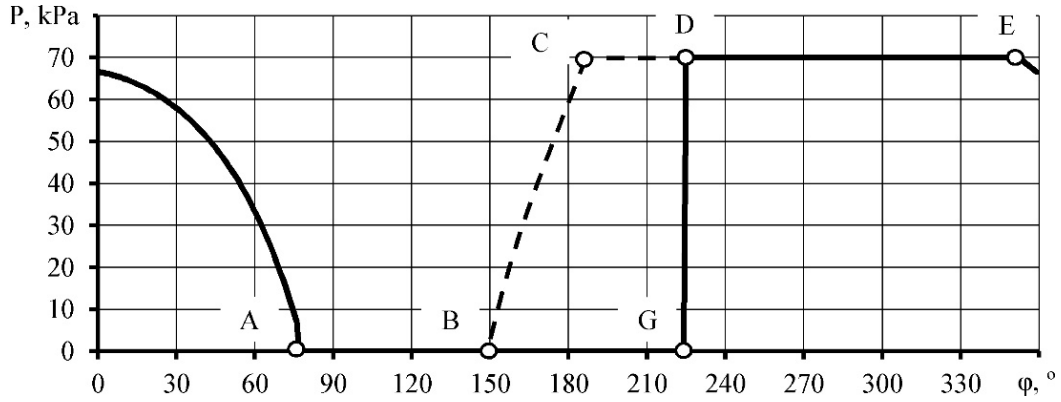


Fig. 3. Analytical dependence of pressure changes in the working chamber of the pump on the rotor rotation angle ($\alpha_{in}$= 72. 8°, $\alpha_{out}$= 56.8°, n = 2200 rpm)

Thus, the pump will have the following calculated parameters of the air distribution phases: suction angle $\alpha_{in}$ = 72.8°; fully compression angle $\alpha_p$ = 174.8°; release angle $\alpha$ = 50.3°; injection angle $\alpha_{out}$ = 56.8°; the angle of harmful space $\delta$ = 58.7°; suction end angle $\varphi_{in}$ = 151.5°.

## 3. Numerical modeling

### 3.1. Methods of numerical modeling

Analysis of previous analytical studies showed that the proposed mathematical model, which describes the working process of the vacuum pump does not fully reflect the actual change in vacuum pressure in the working chamber, as they do not consider internal flows in the pump and changes in thermodynamic air. Therefore, studies of the working process of a rotary vane vacuum pump were performed by the method of numerical modeling using the software package PumpLinx [20]. To perform the modeling, a 3D model grid of a rotary vane vacuum pump was constructed using a surface mesh generator and polyhedral cells (Fig. 4). The basic cell size was 0.001 m.

The modeling was performed using a rotary vane pump model. The movement of air was subject to a turbulent state with possible cavitation. At the initial time, the air in the pump was at atmospheric pressure – 101.325 kPa and temperature – 300 K.

Based on the accepted productivity of the vacuum pump (1200 l/min) and on the results of research [21, 22] the following design parameters were obtained: stator diameter was $D_p$ = 0.1716 m, rotor diameter $d_p$ = 0.146, rotor length $L_p$ =

0.172 m, eccentricity $m_p$ = 0.0128 m, plate thickness $h_p$ = 0.005 m; the number of plates $Z_p$ = 4 (Fig. 1).

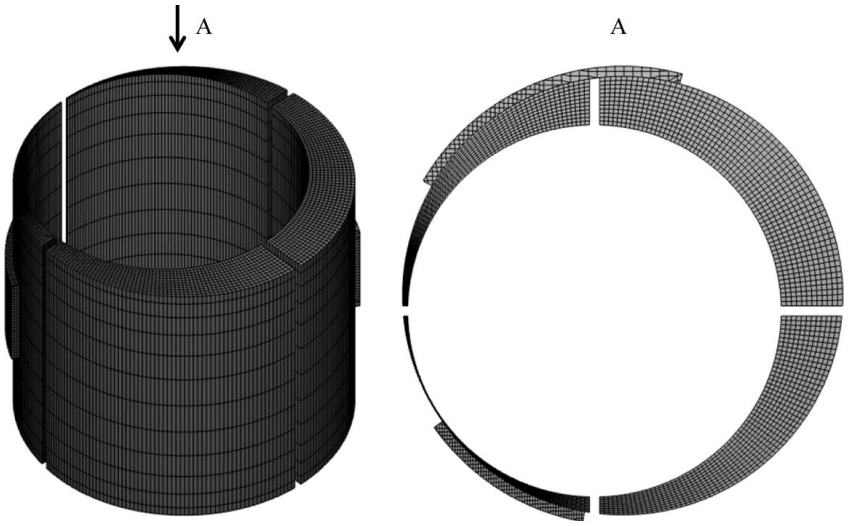


Fig. 4. 3D grid of the model of the rotary vane vacuum pump in the PumpLinx software package

During the simulation, the geometric dimensions of the pump were changed, namely the phases of air distribution: the suction angle of the vacuum pump in the range from 60 to 90, the injection angle of the vacuum pump out in the range from 50 to 70 (Fig. 1). The rotor speed n was changed from 1000 to 3000 rpm.

### 3.2. The results of numerical modeling

As a result of numerical modeling of the working process of a rotary vane vacuum pump, the dynamics of the vacuum pressure distribution were obtained (Fig. 5).

Determination of the vacuum pressure in the working chamber of the pump from the angle of rotation of the rotor (Fig. 5) made it possible to obtain a graph of its change (Fig. 6).

As can be seen from Figs. 6 suction begins with a sharp increase in the curve of vacuum pressure at point G. Then the curve becomes maximum when the working chamber has the largest volume (point E). As the volume of the chamber decreases, during its further movement, the value of the vacuum pressure decreases because of air compression. The pressure at the end of compression in the working chamber should be equal to atmospheric, in fact, it corresponds to point A on the indicator diagram. Therefore, at the time of connection of the chamber with the discharge window, the pressure in the injection space exceeds

the pressure in the compression space. At the time of opening the injection window air from the injections space flows smoothly into the chamber. As a result of overflow, the pressure in the chamber and the discharge window is equalized.

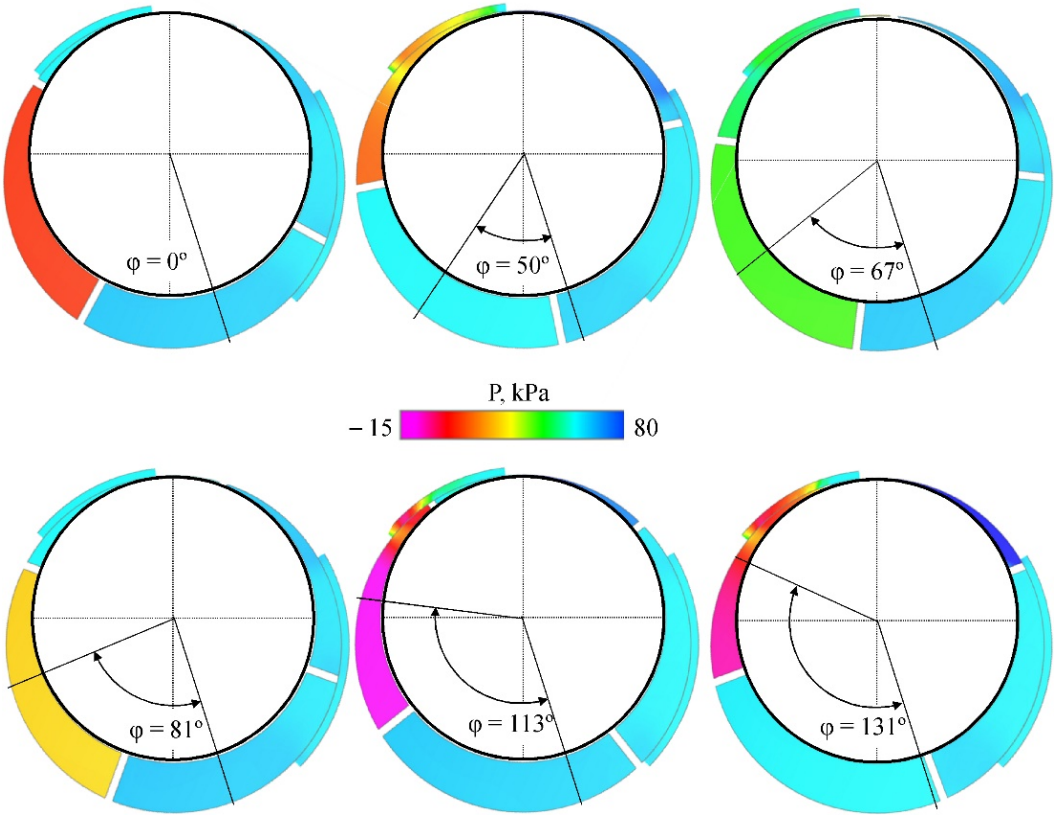


Fig. 5. Dynamics of vacuum pressure distribution of a laminose rotating vacuum pump ($\alpha_{in}$= 72.8°, $\alpha_{out}$= 56.8°, n = 2200 rpm)

As the rotor rotates, the air is expelled because of the chamber volume being reduced. The air is expelled to point F, and with further movement of the rotor, the next chamber is connected to the injection space and the first chamber. Since the second chamber is a vacuum, the pressure in the first chamber decreases to point B. This point corresponds to the position when the pressure in the first and second chambers and in the injections space are equalized. Next, a jump in vacuum pressure is observed on the segment BC'. Then the air is expelled from the second chamber, and this pressure is transmitted to the first chamber, and the pressure in it increases to point H. Although in the second chamber the ejection does not end and the pressure in the discharge space remains from point H, the pressure in the first chamber decreases. The pressure is balanced by the

atmospheric pressure at point G due to the flow of gas between the rotor and the housing.

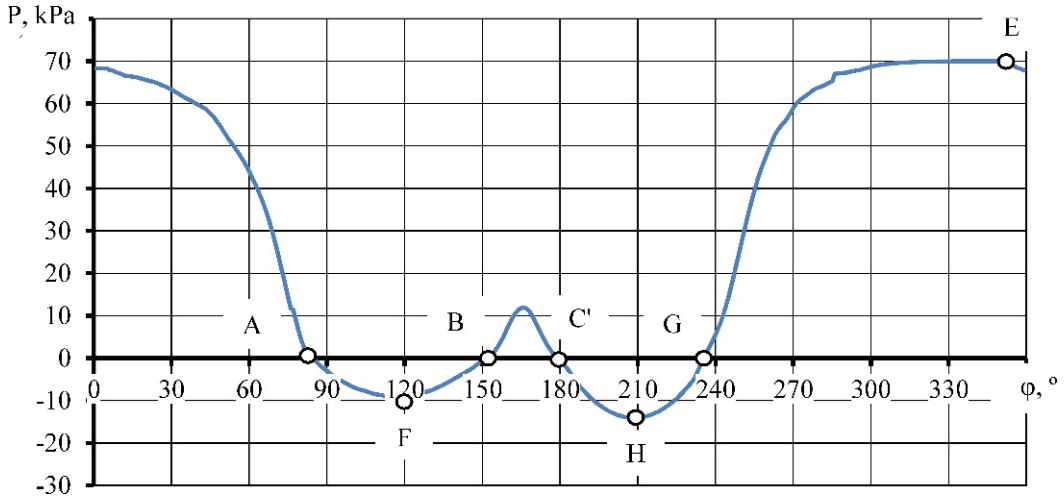


Fig. 6. Numerical dependence of pressure changes in the working chamber of the pump on the rotor rotation angle ($\alpha_{in}$= 72.8°, $\alpha_{out}$= 56.8°, n = 2200 rpm)

## 4. Experimental

### 4.1. Methods of experimental study

To study the phases of air distribution of a rotary vane vacuum pump, it is necessary to determine the dynamic dependencies that characterize the change in vacuum pressure from the angle of rotation of the rotor of the vacuum pump at different speeds.

For research, an experimental sample of a rotary vane vacuum pump with a vacuum pressure sensor was made, the structural scheme of installation of which is presented in Fig. 7. A general view of the manufactured vacuum pump with a vacuum pressure sensor is shown in Fig. 8.

Experimental studies of the air distribution phases of the rotary vane vacuum pump were performed using a stand, which schematic diagram and a general view is shown in Fig. 9.

The speed of the pump rotor n was changed using a Danfoss frequency converter; the value of the vacuum pressure P was set using a flow meter KI-4840M. The values of the vacuum pressure were taken using a sensor MPX5100. The resulting signal was recorded by an oscilloscope Rigol DS1022C, followed by recording the data on a PC (software Ultrascope for DS1000).

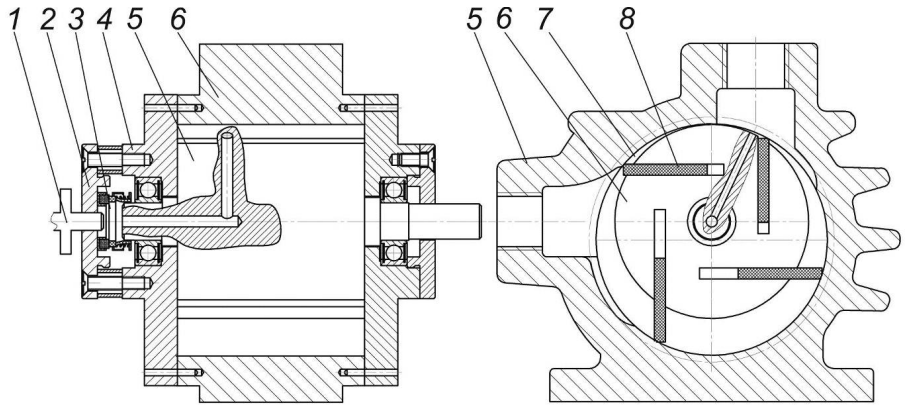


1 – pressure sensor MPX5100; 2 – bearing cover; 3 – end seal; 4 – pump cover; 5 – rotor; 6 – stator; 7 – working chamber; 8 – plates

Fig. 7. Scheme of installation of the pressure sensor in the experimental pump

Fig. 8. General view of the manufactured experimental sample of the plate vacuum pump with the sensor of vacuum pressure

The cavity of the working chamber of the pump was connected to the pressure sensor by means of channels in the body of the rotor.

As a result of experimental studies of the air distribution phases of a rotary vane vacuum pump, dynamic dependences were obtained (Fig. 10). They characterize the change of vacuum pressure in the working chamber as a function of the rotor rotation angle at different rotor rotational speed and vacuum pressure values in the suction window.

Experimental analysis shows that at all these rotational speeds of the rotor, the vacuum pressure varies from the angle of rotation of the rotor with the same frequency. The graphs show that the nature of the dynamic distribution of vacuum pressure is the same at any speed of the rotor. This observation indicates the stability of the experimental rotary vane vacuum pump in different modes.

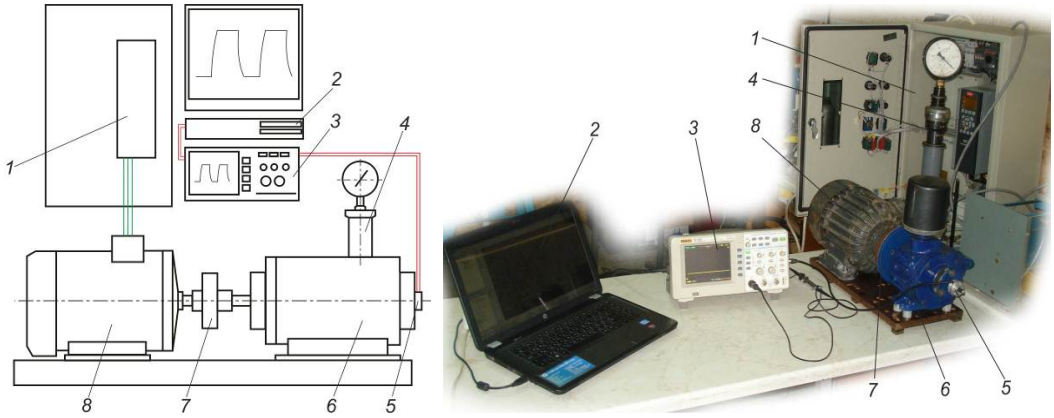


1 – frequency regulator; 2 – PC system unit; 3 – digital oscilloscope Rigol DS1022C;
4 – flow meter KI-4840M; 5 – pressure sensor MPX5100; 6 – experimental vacuum pump;
7 – elastic coupling; 8 – electric motor 4D71V2SU1

Fig. 9. Schematic diagram (a) and General view (b) of the stand for studies of the air distribution phases of the experimental vacuum pump

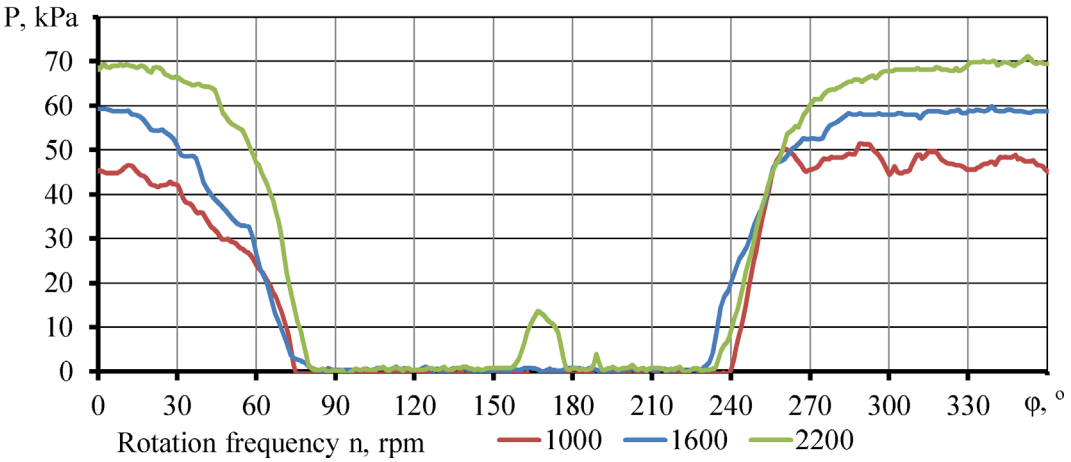


Fig.10. The pressure changes in the pump working chamber as a function of the rotor rotation angle obtained by experimental studies.

## 5. Comparison of research results

To compare the obtained models of the air distribution phases of the rotary vane vacuum pump, the data of analytical studies, numerical modeling, and experimental data are combined (Fig. 11). The experimental data and numerical modeling data corresponding to the level of vacuum pressure adopted in the analytical calculations.

Analyzing the graphs shown in Fig. 11, it can be argued that on the compression and injection side (segment E – A) the deviation of the experimental data and numerical modeling data from the obtained ones is theoretically insignificant. At stages, A – F – B and C – H – G, numerical modeling shows a change in vacuum pressure to a pressure greater than atmospheric. In experimental studies, this is not observed as used sensors of vacuum pressure.

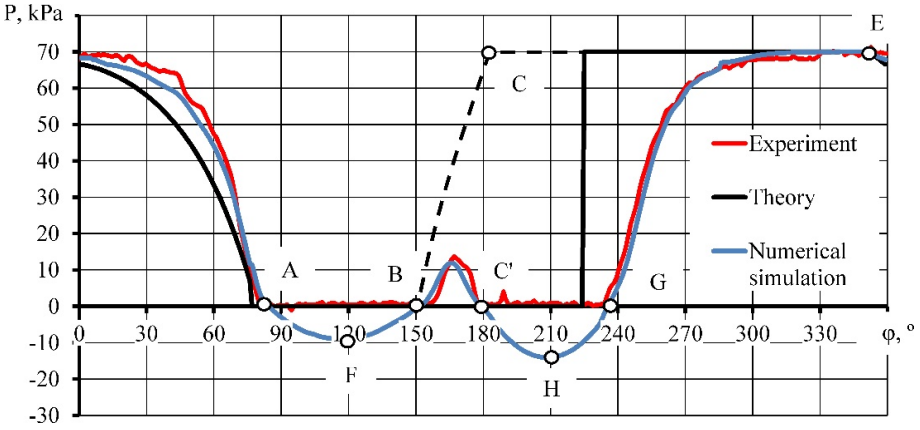


Fig. 11. Comparison of the results of analytical studies, numerical modeling, and experimental data on the dependence of the change in vacuum pressure in the working chamber of the pump on the rotor rotation angle.

On the suction side, which begins after the separation of the chamber (point B), there is a deviation of theoretical and experimental data, the segment B – C, although in nature corresponds to the segment G– E but has a shift in the angle. This is because the channel of the pressure sensor is in the rear, during the rotation of the rotor, part of the chamber, because of this it was not possible to record the change in vacuum pressure in the first half-chamber. As for the pressure surge on the experimental and numerical curves on segment B – C, it can be explained by the flow of air between the half-chambers with increasing pressure differences in them. In general, from the obtained data it can be stated that the calculated theoretically vacuum pressure is in the confidence corridor of experimental studies. According to the calculated coefficient of correlation between data of numerical modeling and experimental research (R = 0.95) and the calculated value of Fisher's criterion $F = 2.09 < F_{0.05}(2, 360) = 3.02$ the theoretical model of phases of distribution of air of the rotary vane vacuum pump is confirmed. This makes it possible to state that the theoretical equation of distribution of vacuum pressure in the working chamber of the pump from the angle of rotation of the rotor is valid at any value of the rotor speed for a given value of vacuum pressure.

At the end of the tests, the vacuum pump, which had the highest failure time (4600 hours), had a vacuum performance of 48 kPa 14.3 $m^3$/h, or 79 % of the original (at the beginning of the test 18 $m^3$/h). The results of micrometering of parts of this pump are presented in Table 1. Photographs of the details of the vacuum pump are presented in Fig. 12.

Table 1 – The results of micrometering of pump parts

| Name details | Parameter | Part size, mm | | Wear, mm | Relative wear, % |
|---|---|---|---|---|---|
| | | before the test | after the tests | | |
| Plate | thickness | 5.00 | 4.84-4.92 | 0.08-0.16 | 1.6-3.2 |
| | length | 84.90 | 84,85-84.88 | 0.02-0,05 | 0.02-0.05 |
| | height | 41.50 | 41.46-41.48 | 0.02-0.04 | 0.04-0.1 |
| Back cover | thickness | 15.10 | 14.98 | 0.12 | 0.8 |
| Front cover | thickness | 15.12 | 15.02 | 0.10 | 0.6 |
| Stator | diameter | 105.07 | 105.09 | 0.02 | 0.01 |
| Rotor | diameter | 88.03 | 88.03 | – | – |

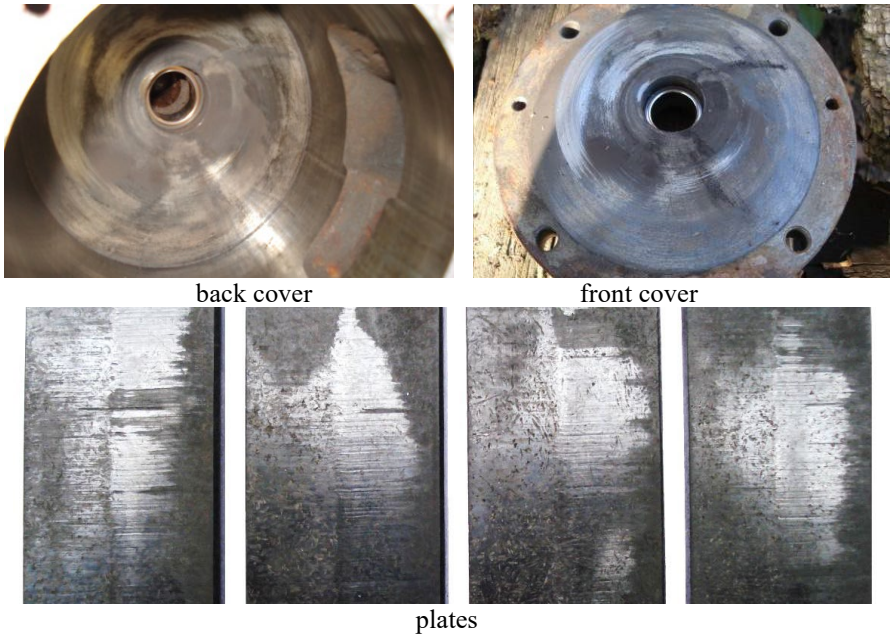


Fig. 12. Details of the developed vacuum pump after production tests as a part of individual milking installation.

## 6. Conclusions

The paper deals with determining the influence of the design and technological parameters of a small-sized rotary vane vacuum pump for mobile

equipment (for example, individual milking machines) on the efficiency of its operation. The improved methodology (and it experimental testing) for determining the parameters of the air distribution phases in such a vacuum pumps with an inclined arrangement of the plates is suggested.

Analytical studies allowed to calculate exactly the cross-section area of working chamber of the plate rotary vacuum pump and to determine the dimensions and location of the suction and discharge windows are determined: suction angle $\alpha_{in}$ = 72.8°; fully compression angle $\alpha_p$ = 174.8°; release angle $\alpha$ = 50.3°; injection angle $\alpha_{out}$= 56.8°; the angle of harmful space $\delta$ = 58.7°; suction end angle $\varphi_{in}$= 151.5°.

Experimental studies of the air distribution phases in vacuum pump allowed to obtained dynamic dependences which characterize the change of vacuum pressure depending on the rotor rotation angle at different rotor rotational speed.

Detailed comparison of analytical research, numerical modeling, and experimental studies and calculated correlation coefficient and Fisher's criterion value confirm the theoretical model of air distribution phases of the rotary vacuum pump.

## R E F E R E N C E S


[1]. *H. Wycliffe*, Rotary pumps and mechanical boosters – as used on today's high vacuum systems, Vacuum, 37 (1987) 603–607, DOI: 10.1016/0042-207X(87)90044-3.

[2]. *Wolfgang Jorisch*, Mechanical Vacuum Pumps, Vacuum Technology in the Chemical Industry, (2014) 97–128, DOI: 10.1002/9783527653898.ch5

[3]. *M.H. Hablanian, E. Bez, J.L. Farrant*, Elimination of backstreaming from mechanical vacuum pumps, Journal of Vacuum Science & Technology A Vacuum Surfaces and Films 5(4) (1987) 2612–2615, DOI: 10.1116/1.574396.

[4]. *E. Bez, D. Guarnaccia, M. Hablanian*, A new oil-free mechanical vacuum pump, AIP Conference Proceedings 171(1) (1988) 262–267, DOI: 10.1063/1.37315.

[5]. *Y. Zhang, H. Huang, C. Li*, Digitization of pumping speed curves of rotary vacuum pump. 34 (2014) 798–801, DOI: 10.3969/j.issn.1672-7126.2014.08.05.

[6]. *M. Azam, M. Umar, Muhammad Maqsood, Akhtar Imran, Imran Aziz*, Pumping Speed Measurement of the Rotary Vane Vacuum Pump by Using Numerical and Experimental Approaches, ASME International Mechanical Engineering Congress and Exposition, Proceedings (IMECE), (2014), DOI: 7. 10.1115/IMECE2014-38412.

[7]. *Uchida Masato, Ishida Shuichi, Tabaru Tatsuo, Miyamoto Hiroyuki,* Anomaly Detection of Rotary Vacuum Pump Using Thin AE Sensor and Reconstruction Error of Autoencoder, Transactions of the Society of Instrument and Control Engineers, 54 (2018) 599–605, DOI: 10.9746/sicetr.54.599.

[8]. *V.P. Khlumsky*, Rotary compressors and vacuum pumps, M.: Mechanical Engineering, (1971) 125.

[9]. *S.I. Pavlenko, V.Yu. Dudin, M.V. Kolonchuk, D.F. Kolga*, Substantiation of some parameters of laminose vacuum pumps, Geotechnical Mechanics: Interdepartmental. zb. Science. Proceedings of the Institute of Geotechnical Mechanics. MS Polyakova NAS of Ukraine, Dnipropetrovsk, Issue. 75 (2008) 258–268.

[10]. *Yu.O. Linnyk, S.I. Pavlenko, E.B. Aliiev*, Experimental studies of the operating parameters of the laminose rotating vacuum pump HB-1200, Bulletin of the Ukrainian Branch of the International Academy of Agrarian Education, Melitopol: Copy Center «Document Service», Issue. 2 (2014) 136–141.
[11]. *V.S. Khmelovsky, S.I. Pavlenko, Yu.O. Linnik, V.Yu Dudin, E.B. Aliiev*, Mechanical and technological bases of use of vacuum pumps of milking installations: monograph, K.: CP «Comprint», (2017) 177, ISBN 978-966-929-645-0.
[12]. *E.B. Aliiev, O.S. Gavrilchenko*, Study of the operation of the blades of the plate-rotor vacuum pump from the duration of its operation, Bulletin of Sumy National Agrarian University, Series "Mechanization and automation of production processes", Sumy, Issue 10/3 (31) (2016) 63–65.
[13]. *A.I. Burya, V.Yr. Dudin*, Investigation of friction and wear of polymer compression materials based on phenol-formaldehyde resin, 6th Interna-tional Symposium INSYCONT'02 "NEW ACHIEVEMENTS in TRIBOLOGY", September 19th-21st, Cracow, Poland, (2002) 243–250.
[14]. *A.O. Pariev, S.I. Pavlenko, S.V. Dubovenko, B.Ю. Dudin,* Pat. 46831 Ukraine, IPC (2009) F04C 2/00. Vacuum plate-rotor pump; applicant and patent owner Institute of Livestock Mechanization UAAS. № in 2009 06676; declared 25.06.2009; public. 11.01.2010, Bull. №1, 2010.
[15]. *N.I. Mzhelsky*, Vacuum pumps for milking installations, M.: Mechanical engineering, (1974) 151.
[16]. *V.I. Elin*, Pumps and compressors, M.: Gostoptekhizdat (1960) 398.
[17]. *Tak Bong-Yeol, Kim Byung-Duk, Yang Hea-Gyeong, Han Gi-Young, Lee So-A.*, Development of Localized Roots Type Medium-Vacuum Pump, Journal of Fluid Machinery, (2011) 14, DOI: 10.5293/KFMA.2011.14.3.023.
[18]. *O. Erenkov, D. Yavorskii, A. Kalenskii*, Improving the Efficiency of a Guarded-Vane Vacuum Pump, Chemical and Petroleum Engineering, (2020) 55, DOI: 10.1007/s10556-020-00727-6.
[19]. *Murakami, Yoshio, Yuyama, Junpei*, Development of an Oil-Free Vacuum Pump using a Unique Bellows, SHINKU, 46 (2003) 185–188, DOI: 10.3131/jvsj.46.185.
[20]. *Lee Seung-Hwan, Jeong Hyun-Yong*, A study on the development of a numerical model for a rotary vane vacuum pump for brake boosters, Journal of Mechanical Science and Technology, 32 (2018) 3677–3685, DOI: 10.1007/s12206-018-0720-9.
[21]. *E. B. Aliev, V. M. Bandura, V. M. Pryshliak, V. M. Yaropud, O. O. Trukhanska*, Modeling of mechanical and technological processes of the agricultural industry, INMATEH – CUPRINS, Vol. 54, Nr. 1 (2018) 95–104.
[22]. *Yu.O. Linnyk, S.I. Pavlenko, E.B. Aliiev, A.B. Gritsun*, Results of numerical modeling of the working process of a laminose rotating vacuum pump of a milking installation, Coll. Sciences, Proceedings of Vinnytsia National Agrarian University, Series: Technical Sciences, Vinnytsia, № 2 (85) (2014) 74–80.
[23]. *V. Yu. Dudin*, Phases of air distribution of a rotating vacuum pump with tangential arrangement of plates, Geotechnical mechanics: Interdepartmental. zb. Science. Proceedings of the Institute of Geotechnical Mechanics. MS Polyakova NAS of Ukraine, Dnipropetrovsk, Issue. 75 (2008) 254-258.